First-principles study of the Young's modulus of Si ⟨001⟩ nanowires

Byeongchan Lee and Robert E. Rudd*

Lawrence Livermore National Laboratory, University of California, L-415, Livermore, California 94551, USA
(Received 3 November 2006; published 16 January 2007)

We report the results of first-principles density functional theory calculations of the Young's modulus and other mechanical properties of hydrogen-passivated Si ⟨001⟩ anowires. The nanowires are taken to have predominantly {100} surfaces, with small {110} facets. The Young's modulus, the equilibrium length, and the residual stress of a series of prismatic wires are found to have a size dependence that scales like the surface area to volume ratio for all but the smallest wires. We analyze the physical origin of the size dependence and compare the results to two existing models.

Nanoscale mechanical devices have been proposed for applications ranging from nanoelectromechanical systems (NEMSs) such as high-frequency oscillators and filters[1] to nanoscale probes[2] to nanofluidic valves[3] to q-bits for quantum computation.[4] The process of design and fabrication of these devices is extremely challenging, complicated in part by uncertainties about how even ideal devices should behave. The mechanical response of nanoscale structures is known to be different than that of their macroscopic analogs and surface effects in these high-surface-to-volume devices are important,[5] but a predictive theory of nanomechanics remains an open problem.

Much of what is known about the mechanics of nanodevices has been learned from atomistic calculations based on empirical potentials. The first such calculations were done for single-crystal α-quartz beams, finding that the Young's modulus decreased with decreasing size.[6,7] These and calculations of the Young's modulus for various other materials have found a size-dependent modulus with an additive correction to the bulk value that scales like the surface area to volume ratio.[8,9] A few studies claim an additional contribution that scales like the edge to volume ratio (cf. Ref. 6), and such a contribution, with a factor of the logarithm of the separation of the edges, has been discussed for epitaxial quantum dots.[10,11] An intuitive way of understanding these effects is that there is a layer of material at the surface (and edges) whose mechanical properties differ from those of the bulk including different elastic moduli and eigenstrains. The formalism of nanoscale mechanics based on the surface energy and its first two strain derivatives (the surface stress and modulus) has been developed.[9,12] Recently it has been proposed that the size dependence of the Young's modulus can be due to the anharmonicity (nonlinearity) of the bulk elastic moduli together with the strain resulting from the surface stress.[13]

To date, experimental data on the size dependence of nanostructure mechanics are very limited. Atomic force microscopy (AFM) measurements of the Young's modulus[14] (E) of cast metallic nanowires show a strong size dependence.[15] Recent experiments have also found a strong size dependence for E of ZnO nanowires[16] and other mechanical properties of ZnO and GaN nanowires.[17] Measurements of E for silica nanobeams have demonstrated that the way in which the beam is clamped (i.e., the boundary conditions) affects the apparent value.[18] A study using a different AFM technique reported a value of E of 18±2 GPa for a <10-nm Si [100] nanowire;[19] for 100–200-nm Si{111} wires, E has been found to be consistent with the bulk value.[20] Experimental challenges measuring the intrinsic nanoscale Young's modulus make this a topic of continued activity, leveraging earlier work on the mechanics of nanotubes.[21]

In the absence of definitive experimental data, first-principles quantum mechanical calculations can provide robust predictions of nanowire mechanical properties, but few results have been reported. One quantum study based on an empirical tight-binding technique has been published.[22] The electronic and optical properties of nanowires have been studied using first-principles techniques, leading to interesting predictions about size-dependent phenomena as evidenced by an increase in band gap due to quantum confinement[23,24] and a switch from an indirect, to a direct, band gap.[25,26] We are not aware of any *ab initio* calculations of nanowire moduli.

Here we present first-principles calculations of the mechanical properties of silicon nanowires, studying the Young's modulus due to its direct relevance to the function of nanoscale devices such as flexural-mode mechanical resonators[1] and as an archetype for a variety of mechanical properties. We address several important open questions in nanomechanics. Can the modulus size dependence seen with empirical potentials be verfied from first principles or are the potentials missing essential physics? What aspects of the electronic bonds dominate the size-dependent mechanical properties? We focus on prismatic Si ⟨001⟩ nanowires with a combination of {100} and {110} H-passivated surfaces and single-crystal cores as in experiment.[1,27] We have chosen the [001] orientation for the longitudinal axis because of its relevance to the NEMS devices;[1] Si nanowires grown rather than etched typically have different orientations.[28] Hydrogen passivation results from rinsing the oxidized Si surfaces with HF, and it provides a standard system suitable for a systematic study of the size dependence in nanomechanics. With other surface conditions the band gap can vary greatly, and nanowires can go from semiconducting to metallic,[29] but the H-passivated wires remain semiconducting[30] and the surfaces do not change the nature of Si-Si chemical bonding from its covalent character.

First-principles density functional theory (DFT) has been employed: specifically, the Vienna *ab initio* simulation package using the projector augmented-wave method[31,32] within
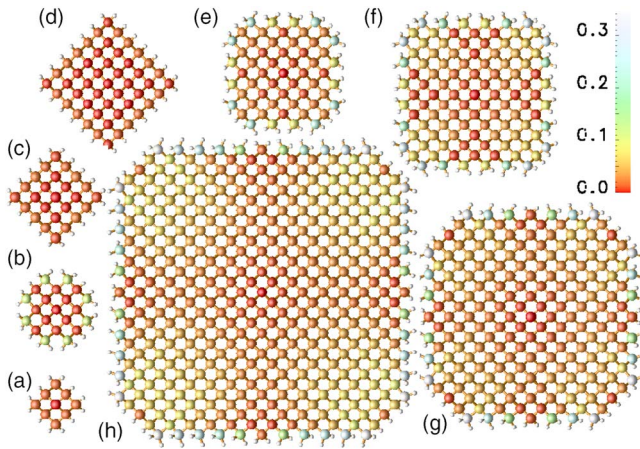
FIG. 1. (Color online) Cross sections of fully relaxed hydrogen-passivated wires, with each Si atom colored as shown in the legend corresponding to its transverse relaxation in Å. The widths of wires are (a) 0.61 (b) 0.92, (c) 1.00, (d) 1.39, (e) 1.49, (f) 2.05, (g) 2.80, and (h) 3.92 nm, respectively. The width is defined as the square root of the cross-sectional area.

the generalized gradient approximation (GGA).[33] The energy cutoff for the plane-wave expansion is 29.34 Ry and higher, and six points in the one-dimensional irreducible Brillouin zone are used for k-point sampling. Each supercell is periodic, is one Si cubic unit cell long along the wire, and has more than 10 Å vacuum space in the transverse directions.

To calculate E, we define the cross-sectional area to be the area bounded by the centers of the outermost (H) atoms. This choice is motivated by the fact that the volume excluded by the wire from access by outside atoms is determined from the forces arising from electron interactions. Most of the electron density is enclosed by the boundary formed by H atoms and the electron density from Si atoms essentially vanishes beyond this point. The positions of the nuclei are well defined and not subjective. Other definitions of the bounding surface exist: for example, the midplane between two identical H-passivated surfaces at their minimum energy separation.[34]

The cross-sectional shape of the Si [001] wire is a truncated square with four {100} facets and four {110} facets. Some wires studied have no {100} facets; for those that do, the ratio of the facet areas is taken to be roughly in accordance with the Wulff shape for a bare wire with (110)-(1×1) and (100)-$p(2\times2)$ surface reconstructions; i.e., the ratio of {100} to {110} area is 3.5:1. For each of the nanowire geometries shown in Fig. 1, the Si atoms were initially positioned at their bulk lattice sites and hydrogen atoms were added to terminate the bonds at the surfaces. On the {100} facets the H atoms were added in a dihydride configuration preferred over monohydride at low temperature.[35] The system was then relaxed to its zero-temperature minimum energy with the length of the periodic supercell held fixed at the bulk value in the longitudinal direction. The axial stress in this configuration, $\sigma_{zz}(L_0) = V^{-1}\partial U/\partial\epsilon_{zz}|_0$, where U is the DFT total energy, is indicative of the residual stress in a doubly clamped beam etched from a single-crystal substrate. It is plotted in Fig. 2.
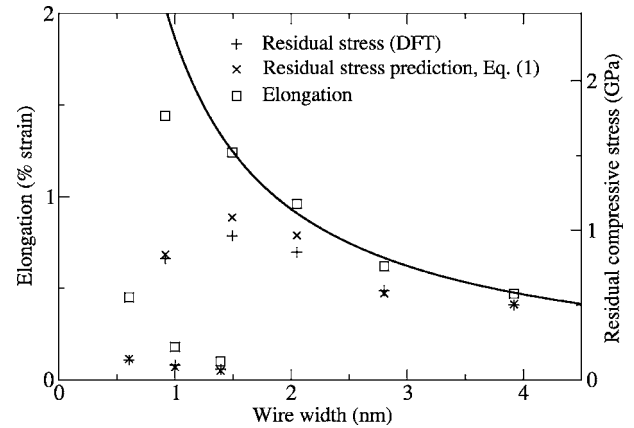

FIG. 2. Silicon nanowire axial stress and equilibrium elongation strain calculated in DFT as a function of wire size. The solid curve is a fit to C/w of the elongation strain to 4 data points from 1.49 nm and larger wires, with $C=1.9\%$ nm. The predictions of Eq. (1) are also plotted using the stresses from DFT calculations of hydrogenated 14-layer {100} and 15-layer {110} slabs. The asterisklike symbols are from overlaps.

Next the relaxed total energy was calculated for each wire in a series of longitudinal strains at increments of roughly 0.5%. These total energy values were fit to a polynomial. The minimum of the polynomial gives the equilibrium length, and the value of the curvature at the minimum gives the Young's modulus, $E = V^{-1}\partial^2U/\partial\epsilon_{zz}^2|_{\epsilon_{zz-min}}$. The equilibrium elongation and modulus are plotted in Figs. 2 and 3, respectively.

The calculated Young's modulus of the 1.49-nm wire is tabulated in Table I. The table gives an indication of the sensitivity to the order of the polynomial fit. For the given order, a higher cutoff energy offers little improvement. We find that the second-order fit with 29.34 Ry energy cutoff is reasonably good, differing by less than 2% compared with all
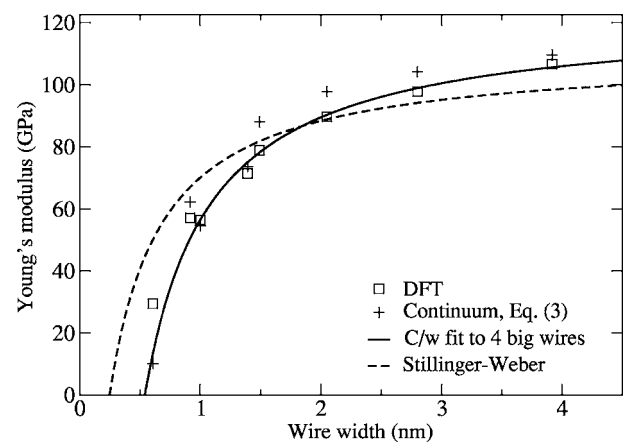

FIG. 3. Silicon nanowire Young's modulus calculated in DFT as a function of wire size. For comparison values of continuum formula (3) are also plotted, using the {100} and {110} surface elastic constants obtained in DFT from hydrogenated 14-layer {100} and 15-layer {110} slabs, respectively. The solid curve $E=E_{bulk}^{DFT}-C/w$, with $C=66.11$ GPa/nm, is the best fit to a pure surface area to volume size dependence.

TABLE I. The calculated Young's modulus in GPa of the 1.49-nm nanowire as a function of the plane-wave cutoff energy and the order of the fit. The same ten data points were fit for each polynomial order.

Cutoff energy (Ry)	Order of polynomial fitting				
	Second	Third	Fourth	Fifth	Sixth
29.34	78.90	78.88	79.90	79.94	78.61
44.10	79.31	79.28	80.39	80.33	78.95
51.45	79.40	79.37	80.35	80.31	79.01

the higher-order combinations tested. The second-order fit also permits direct comparison with the results from larger wires where the number of data points and the energy cutoff are limited by the computational cost of systems up to 405 Si and 100 H atoms.

These calculations allow us to analyze the physical origin of the size dependence. Size dependences of the residual stress and the elongation evident in Fig. 2 are driven by the same physics: compressive surface stress. The residual axial stress of the Si beam may be decomposed into core, H adatom and Si surface parts: core contributions from the Si atoms, extrinsic contributions from hydrogen (H-H) interactions, and intrinsic surface contributions from the change to the Si bonds near the surface compared to the Si bulk (Si-H and modified bond order Si-Si). Since DFT only provides a total energy, this decomposition is somewhat ambiguous. We estimate the H-H interactions as equal to those of neighboring hydrogens in two silane molecules in the orientation and separation of the H-passivated surface and the core contribution to be the axial stress in bulk Si uniformly strained to match the nanowire; the intrinsic contribution is the remainder. The extrinsic contribution is most important, as we now show. The intrinsic surface stress is small, as expected since the dangling Si bonds are well terminated with H and the Si-Si bond order is not significantly different than in the bulk. The small magnitude of the intrinsic stress is best seen in the case of the 1.39-nm wire for which the elongation is less than 0.1% compared to ~1.5% of the 1.49-nm wire. The absence of {100} facets on this wire leads to a small extrinsic stress since the H-H separation on the {110} facets is relatively large. The vacant Si sites above the facets are filled by one and two H atoms on {110} and {100}, respectively, and the double occupancy, albeit with ~2 Å H-H separation due to the shorter Si-H bond, leads to more repulsion for {100}.[36]

The extrinsic surface stress due to the H-H repulsion on the {100} facets quantitatively accounts for both the compressive residual stress $\sigma_{zz}(L_0)$ and the elongated equilibrium length L_{eq} of the nanowires. They are related to leading order through the linear elasticity:

$$\sigma_{zz}(L_0) = \sigma_{zz}(\text{core}) + \frac{1}{A}\sum_i \tau_{zz}^{(i)} w_i, \qquad (1)$$

$$(L_0 - L_{eq})/L_{eq} \sim \sigma_{zz}(L_0)/E, \qquad (2)$$

where A is the cross-sectional area, w_i is the width, $\tau_{zz}^{(i)}$ is the longitudinal surface stress of facet i, and L_0 is the bulk length

of the beam. E is the Young's modulus of the beam. For constant surface stress, the second term in Eq. (1) is proportional to the surface area to volume ratio; the core stress is too, since the surface stress causes a transverse expansion of the wire that induces a tensile core stress. We now use much smaller periodic slabs to quantify these contributions and compare with the nanowire results. Using H-passivated slabs we calculate in DFT the surface stress of the ground-state canted (100) surface to be −55.0 meV/Å^2 and that of the (110) surface to be −1.3 meV/Å^2.[37] The negative stress indicates compression. The core stress may be estimated through a generalized Young-Laplace law to be $\sigma_{zz}(\text{core}) \approx -8\nu\tau_{zz}^{\{100\}}/\pi w$, where $\nu = C_{12}/(C_{11}+C_{12})$ is the Poisson ratio. The details of these calculations will be given elsewhere.[36] Using these values in Eq. (1) gives predictions in very good agreement with the full nanowire calculations as shown in Fig. 2. The scatter for 1.49- and 2.05-nm wires may be accounted for by small edge effects. The 0.61-, 1.00-, and 1.39-nm wires have no {100} facets and almost no elongation as described above. In the case of the second smallest (0.92 nm) wire all of the {100} atoms undergo substantial relaxation, as shown in Fig. 1, lowering the magnitude of the surface stress and the elongation. This high level of agreement gives us confidence that we understand the physics of the size dependence of the residual stress.

What about the Young's modulus? As shown in Fig. 3, it softens monotonically from the bulk value ($E_{bulk}^{\text{DFT}} = 122.53$ GPa) in proportion to the surface area to volume ratio. It does not exhibit a strong dependence on the ratio of the {100} to {110} area seen in the equilibrium length. As with the residual stress, the Young's modulus may be decomposed into intrinsic, core, and extrinsic contributions. From continuum mechanics neglecting edge and nonlocal effects, the modulus can be expressed, slightly generalizing Ref. 9, as

$$E = E(\text{core}) + \frac{1}{A}\sum_i S^{(i)} w_i, \qquad (3)$$

where $S^{(i)}$ is the surface elastic constant, a strain derivative of the surface stress including both extrinsic and intrinsic parts. The insensitivity to the facet ratio suggests several conclusions: The extrinsic contribution to the modulus (which is strongly facet dependent) is small, the core anharmonicity is irrelevant since the modulus is not correlated with the equilibrium elongation, and the intrinsic surface contribution dominates and its {100} value may be nearly sufficient to determine E. To study the core stress further, we calculated that the Young's modulus of the bulk crystal increases by only 1.6% when strained ~1.5% to match the most strained (0.92-nm) wire. This change is negligible compared to the observed softening (contrary to claims that the bulk anharmonicity is dominant[13]). The extrinsic effect is also small, but not negligible. Based on silane interaction forces for the canted {100} surface geometry we have estimated that the extrinsic contribution is ~8 GPa for the 1.49-nm wire,[36] roughly equal to $E(1.49 \text{ nm}) - E(1.39 \text{ nm})$—i.e., the difference in the moduli with and without {100} facets. We have also calculated the size dependence of the modulus using Eq.

([3](#)) based on the surface elastic constant $S^{\{100\}}$ from a separate slab calculation.[36] The results, shown in Fig. [3](#), are in good agreement with the full first-principles calculation, and adding the core contribution slightly improves the agreement. Also plotted in the figure is the best fit curve of Ref. [9](#) from Stillinger-Weber (SW) empirical molecular statics calculations. The SW bulk Young's modulus is 13% lower and the coefficient C of the $1/w$ term is 29% lower than the DFT values. The errors compensate for each other, leading to reasonable agreement for the nanoscale wires, which is unexpected since the SW potential does not have the relevant nanophysics in its functional form or its fitting database.

In conclusion we have calculated the size dependence of the Young's modulus and other mechanical properties of silicon nanowires from first principles. In each case the size dependence scales roughly as the surface area to volume ratio, as observed previously with empirical potentials. Analysis based on the first-principles calculations has shown different reasons for the size dependence. For the equilibrium length and residual stress it is due to the extrinsic surface stress from interactions in the H passivation layer; for the Young's modulus, it arises from the intrinsic contribution to the surface elastic constant. Surface parameters from slab calculations capture most, but not all, of the physics. The size effect is not strong for the H-terminated surfaces studied here: the Young's modulus is softened by about 50% for a 1-nm-diam wire. It may be possible to measure this effect directly using either AFM deflection or resonant frequency measurements in a double clamped configuration. Another interesting possibility is that the effect could be substantially stronger in Si nanowires with different surfaces, such as bare or oxide surfaces, making measurements easier. For those systems, the balance of core, intrinsic, and extrinsic contributions could be different, and indeed, new functional forms may be needed for the smallest wires.

*Electronic address: robert.rudd@llnl.gov

[1] A. N. Cleland and M. L. Roukes, Appl. Phys. Lett. **69**, 2653 (1996).

[2] C. L. Cheung, J. H. Hafner, and C. M. Lieber, Proc. Natl. Acad. Sci. U.S.A. **97**, 3809 (2000).

[3] S. D. Solares, M. Blanco, and W. A. Goddard, Nanotechnology **15**, 1405 (2004).

[4] A. N. Cleland and M. R. Geller, Phys. Rev. Lett. **93**, 070501 (2004).

[5] J. W. Cahn, Acta Metall. **28**, 1333 (1980).

[6] J. Q. Broughton, C. A. Meli, P. Vashishta, and R. K. Kalia, Phys. Rev. B **56**, 611 (1997).

[7] R. E. Rudd and J. Q. Broughton, J. Mod. Sim. Microsys. **1**, 29 (1999).

[8] R. E. Rudd, Int. J. Multiscale Comp. Eng. **2**, 203 (2004).

[9] R. E. Miller and V. B. Shenoy, Nanotechnology **11**, 139 (2000).

[10] V. A. Shchukin, N. N. Ledentsov, P. S. Kop'ev, and D. Bimberg, Phys. Rev. Lett. **75**, 2968 (1995).

[11] R. E. Rudd, G. A. D. Briggs, A. P. Sutton, G. Medeiros-Ribeiro, and R. S. Williams, Phys. Rev. Lett. **90**, 146101 (2003).

[12] R. V. Kukta, D. Kouris, and K. Sieradzki, J. Mech. Phys. Solids **51**, 1243 (2003).

[13] H. Liang, M. Upmanyu, and H. Huang, Phys. Rev. B **71**, 241403(R) (2005).

[14] E. W. Wong, P. E. Sheehan, and C. M. Lieber, Science **277**, 1971 (1997).

[15] S. Cuenot, C. Fretigny, S. Demoustier-Champagne, and B. Nysten, Phys. Rev. B **69**, 165410 (2004).

[16] C. Q. Chen, Y. Shi, Y. S. Zhang, J. Zhu, and Y. J. Yan, Phys. Rev. Lett. **96**, 075505 (2006).

[17] G. Feng, W. D. Nix, Y. Yoon, and C. J. Lee, J. Appl. Phys. **99**, 074304 (2006).

[18] X. Q. Chen, S. L. Zhang, G. J. Wagner, W. Q. Ding, and R. S. Ruoff, J. Appl. Phys. **95**, 4823 (2004).

[19] T. Kizuka, Y. Takatani, K. Asaka, and R. Yoshizaki, Phys. Rev. B **72**, 035333 (2005).

[20] A. San Paulo, J. Bokor, R. T. Howe, R. He, P. Yang, D. Gao, C. Carraro, and R. Maboudian, Appl. Phys. Lett. **87**, 053111 (2005).

[21] J. Bernholc, D. Brenner, M. B. Nardelli, V. Meunier, and C. Roland, Annu. Rev. Mater. Sci. **32**, 347 (2002).

[22] S. Ismail-Beigi and T. Arias, Phys. Rev. B **57**, 11923 (1998); D. E. Segall, S. Ismail-Beigi, and T. A. Arias, *ibid.* **65**, 214109 (2002).

[23] A. J. Read, R. J. Needs, K. J. Nash, L. T. Canham, P. D. J. Calcott, and A. Qteish, Phys. Rev. Lett. **69**, 1232 (1992).

[24] B. Delley and E. F. Steigmeier, Appl. Phys. Lett. **67**, 2370 (1995).

[25] X. Zhao, C. M. Wei, L. Yang, and M. Y. Chou, Phys. Rev. Lett. **92**, 236805 (2004).

[26] T. Vo, A. J. Williamson, and G. Galli, Phys. Rev. B **74**, 045116 (2006).

[27] A. Gaidarzhy, G. Zolfagharkhani, R. L. Badzey, and P. Mohanty, Phys. Rev. Lett. **94**, 030402 (2005).

[28] C. M. Lieber, MRS Bull. **28**, 486 (2003).

[29] R. Rurali and N. Lorente, Phys. Rev. Lett. **94**, 026805 (2005).

[30] D. D. D. Ma, C. S. Lee, F. C. K. Au, S. Y. Tong, and S. T. Lee, Science **299**, 1874 (2003).

[31] P. E. Blöchl, Phys. Rev. B **50**, 17953 (1994).

[32] G. Kresse, and D. Joubert, Phys. Rev. B **59**, 1758 (1999).

[33] J. P. Perdew, K. Burke, and M. Ernzerhof, Phys. Rev. Lett. **77**, 3865 (1996).

[34] K. Stokbro, E. Nielsen, E. Hult, Y. Andersson, and B. I. Lundqvist, Phys. Rev. B **58**, 16118 (1998).

[35] S. Ciraci and I. P. Batra, Surf. Sci. **178**, 80 (1986).

[36] B. Lee and R. E. Rudd (unpublished).

[37] For comparison we calculate the {100} and {110} surface energies to be 19.6 meV/Å^2 and 8.2 meV/Å^2, respectively.